

Intermolecular hydrogen bonding assisted aggregation induced emission in quinolone–quinazoline conjugates and their potential use in acidochromism

Irshad Ali,^{a+} Bhupendra Kumar Dwivedi,^{a,b+} Vishwa Deepak Singh,^a and Daya Shankar Pandey^{a*}

Department of Chemistry, Institute of Science, Banaras Hindu University, Varanasi–221005, India

Contents

Page. No.		Page
3.	¹ H and ¹³ C NMR spectra of A1	S1
4.	¹ H and ¹³ C NMR spectra of A2	S2
5.	¹ H and ¹³ C NMR spectra of A3	S3
6.	¹ H and ¹³ C NMR spectra of Q1	S4
7.	¹ H and ¹³ C NMR spectra of Q2	S5
8.	¹ H and ¹³ C NMR spectra of Q3	S6
9.	IR spectra of A1 , A2 and A3	S7
10.	IR spectra of Q1 , Q2 and Q3	S8
11.	HRMS spectra of Q1 and Q2	S9
12.	HRMS spectra of Q3	S10
12.	Solid–state emission spectrum of Q1 , Q2 and Q3	S11
13.	Absorption spectra of Q1 , Q2 , Q3 and emission spectrum of Q1	S12
13.	Plots between ; Stokes shift vs. Δf and Stokes shift vs. E_T (30)	S13
14.	Absorption spectra of Q1 , Q2 and Q3 in THF/water	S14
14.	Emission spectra of Q2 and Q3 in THF/water	S15
15.	A logarithmic view of the time–resolved fluorescence of Q2 (a), Q3 (b) in THF/water mixture (c = 50 μ M).	S16
15.	Powder XRD Pattern of Q2 .	S17
15.	SEM images of Q2 and Q3 .	S18
16.	DLS spectra of Q2 and Q3 .	S19
16.	Emission spectra of Q1 , Q2 and Q3 in methanol/glycerol.	S20
17.	Crystal packing through π – π stacking	S21

17.	Absorption and Emission spectrum of Q1 , Q1+TFA and Q1+TFA+TEA	S22
18.	Absorption and Emission spectrum of Q2 , Q2+TFA and Q2+TFA+TEA	S23
18.	(a) Emission spectrum of Q3, with TFA titration (b) pKa calculation for Q3 and (c)quantitative relationship between emission intensity and TFA concentration of Q1-Q3	S24
19.	Frontier Molecular orbital of protonated Q3 .	S25
19-23.	Tables.	S1-S9

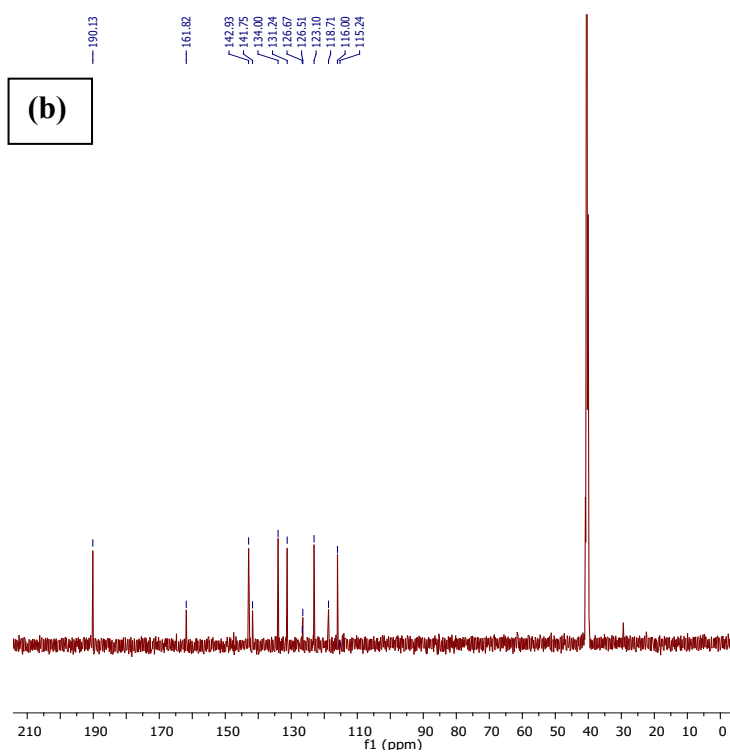
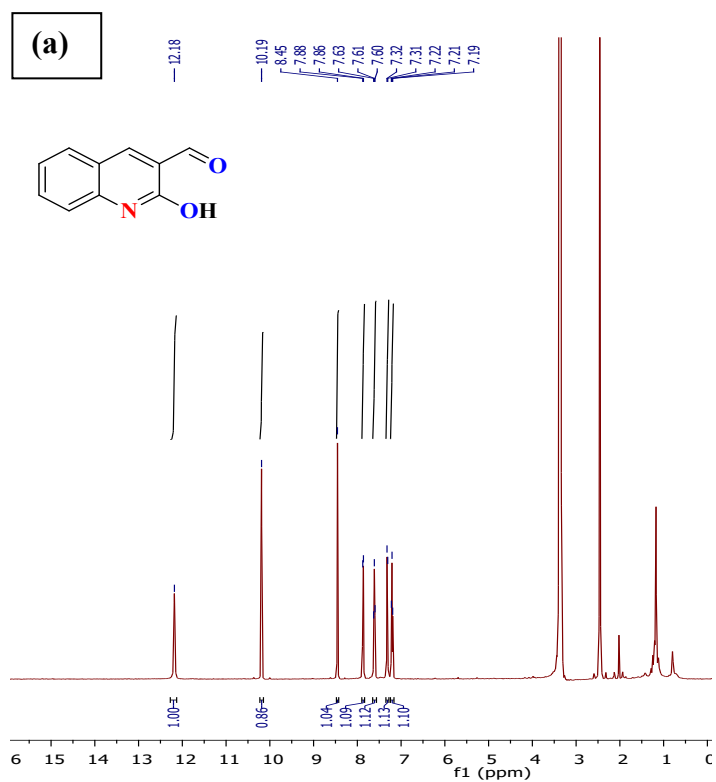


Fig. S1 ^1H (a) and ^{13}C (b) NMR spectra of **A1**.

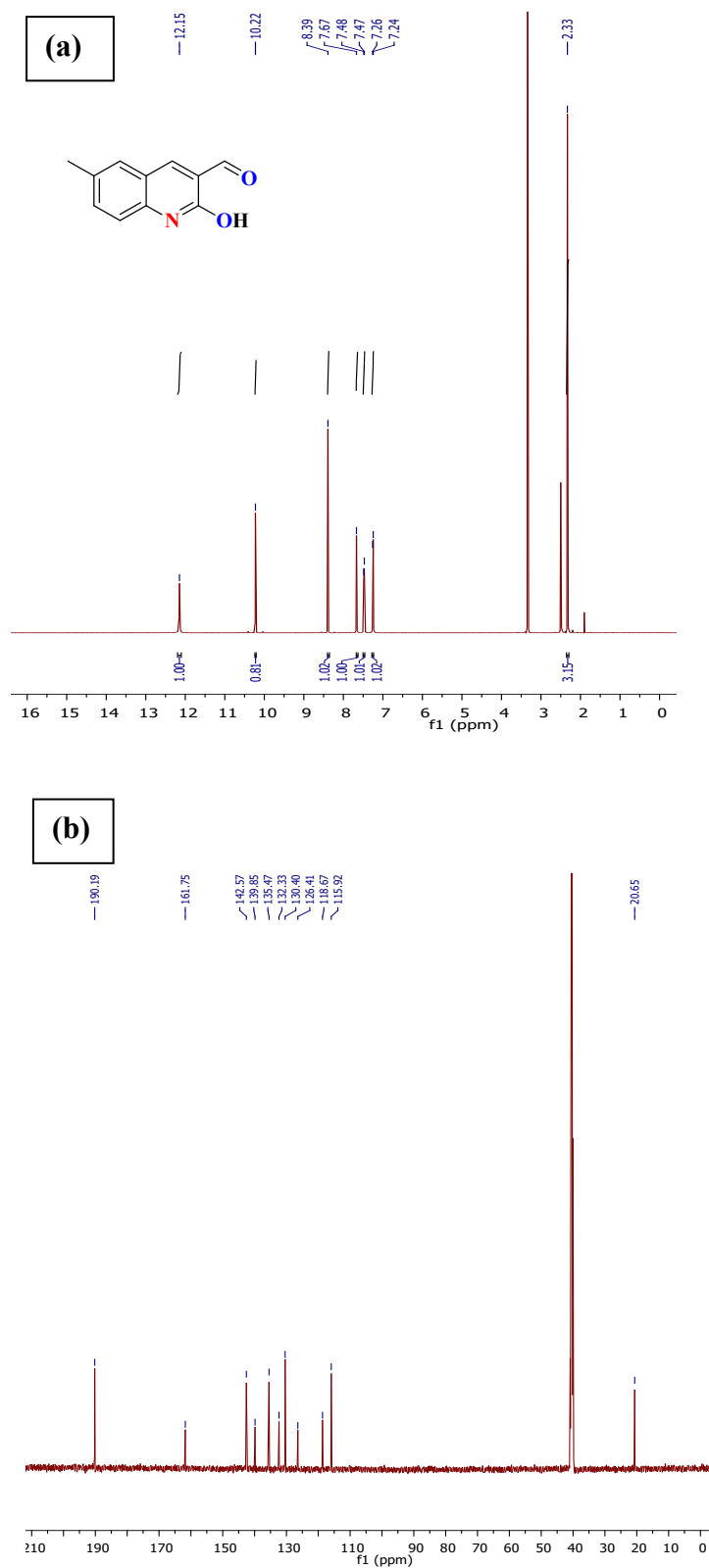


Fig. S2 ^1H (a) and ^{13}C (b) NMR spectra of **A2**.

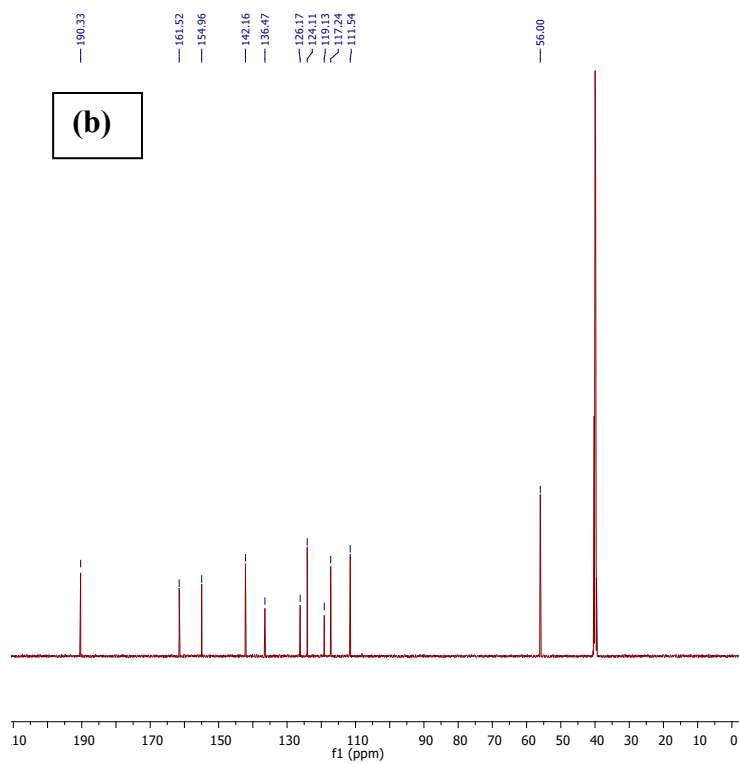
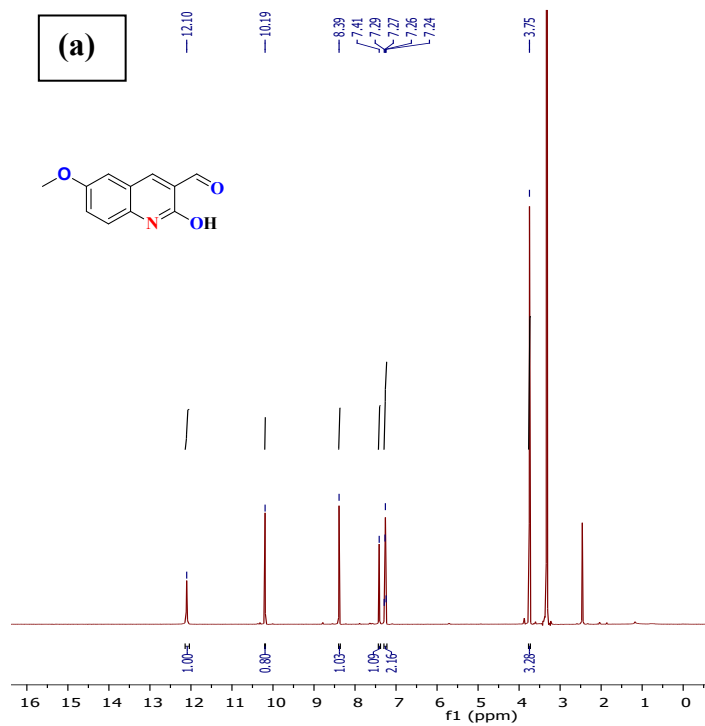


Fig. S3 ^1H (a) and ^{13}C (b) NMR spectra of **A3**.

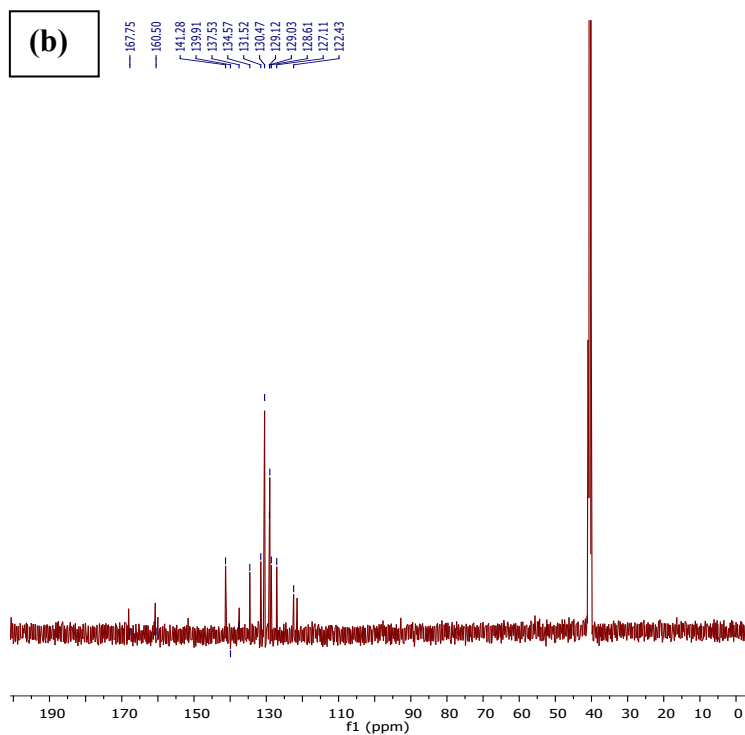
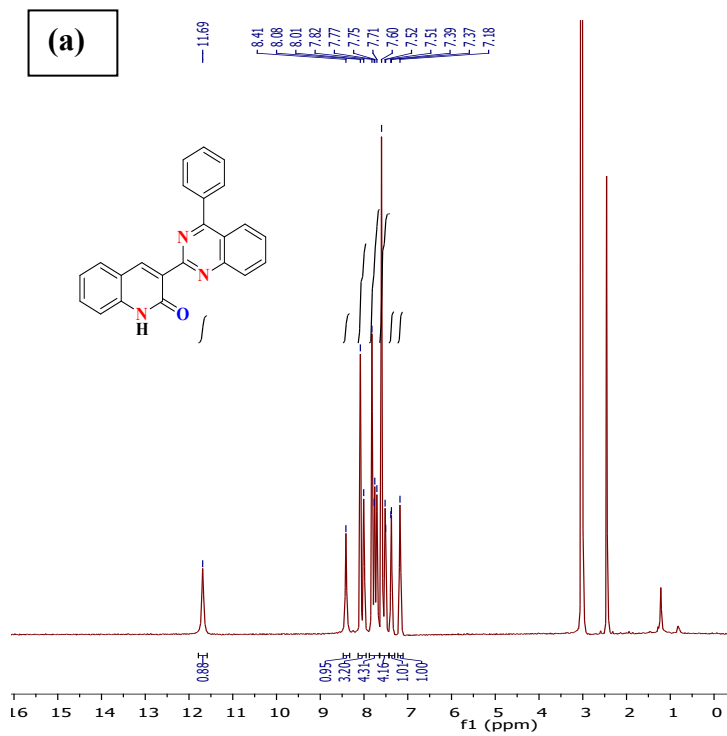


Fig. S4 ^1H (a) and ^{13}C (b) NMR spectra of **Q1**.

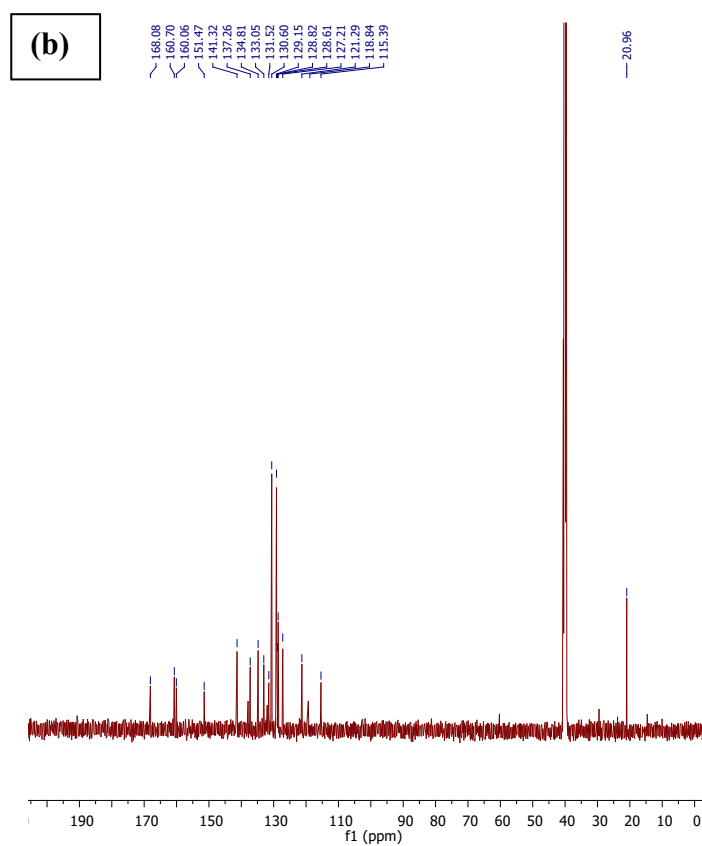
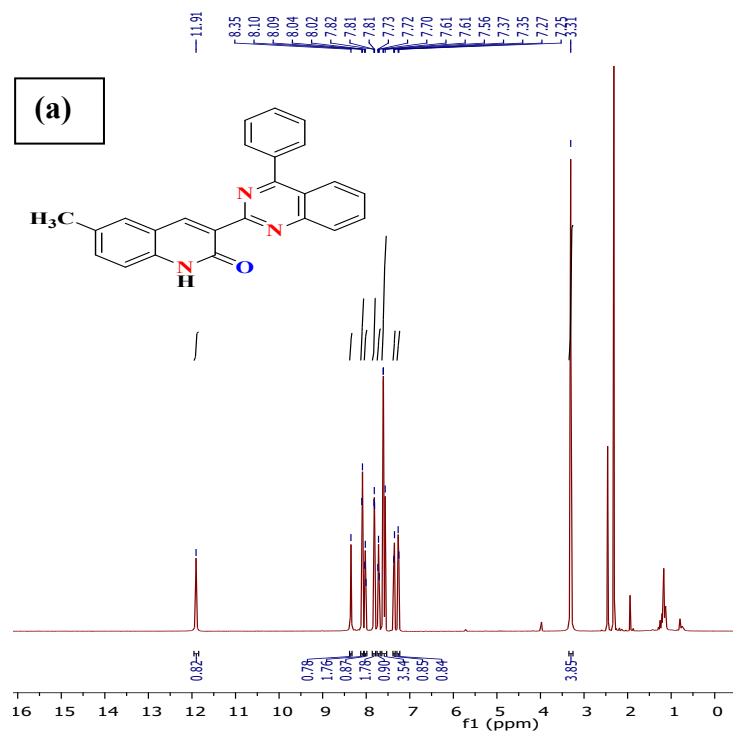


Fig. S5 ^1H (a) and ^{13}C (b) NMR spectra of Q2.

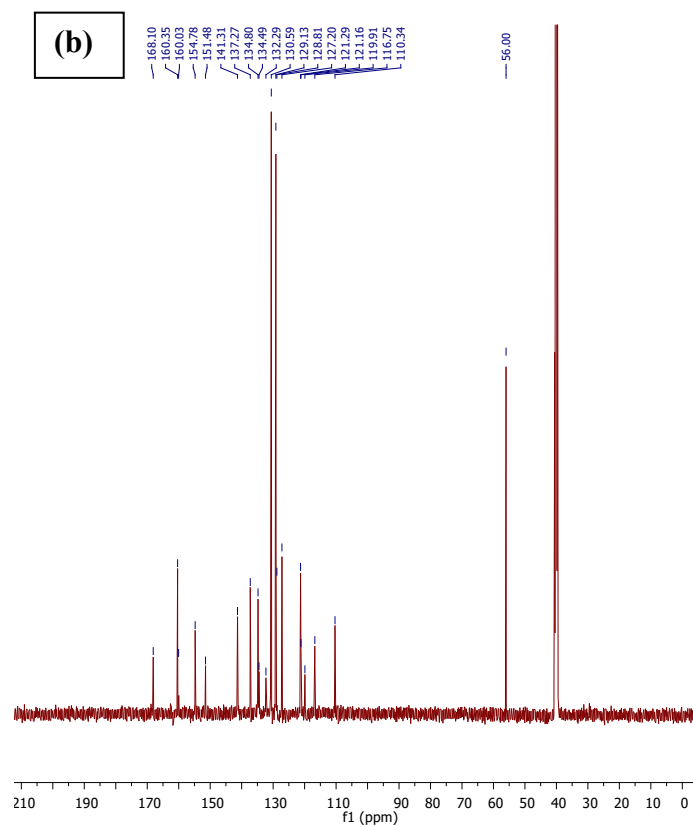
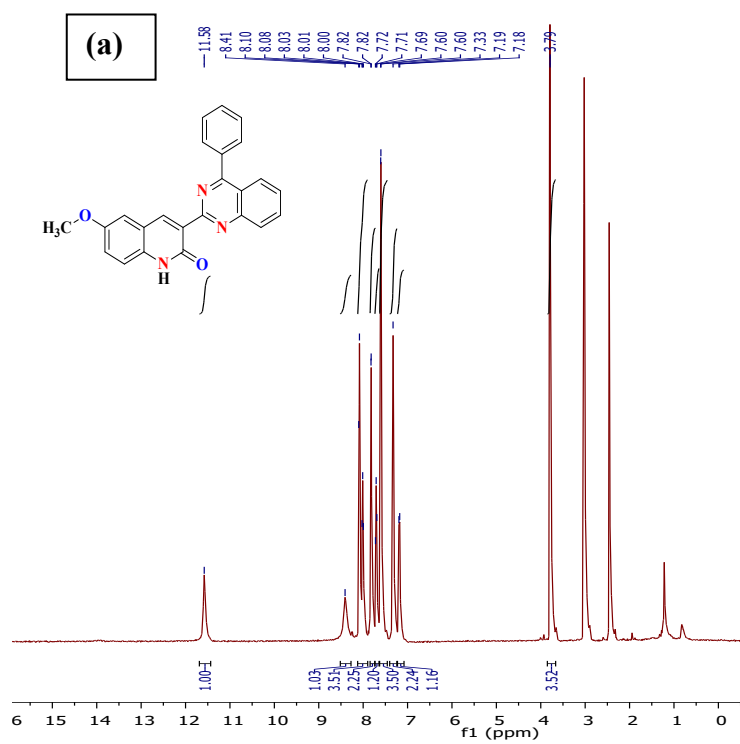


Fig. S6 ^1H (a) and ^{13}C (b) NMR spectra of Q3.

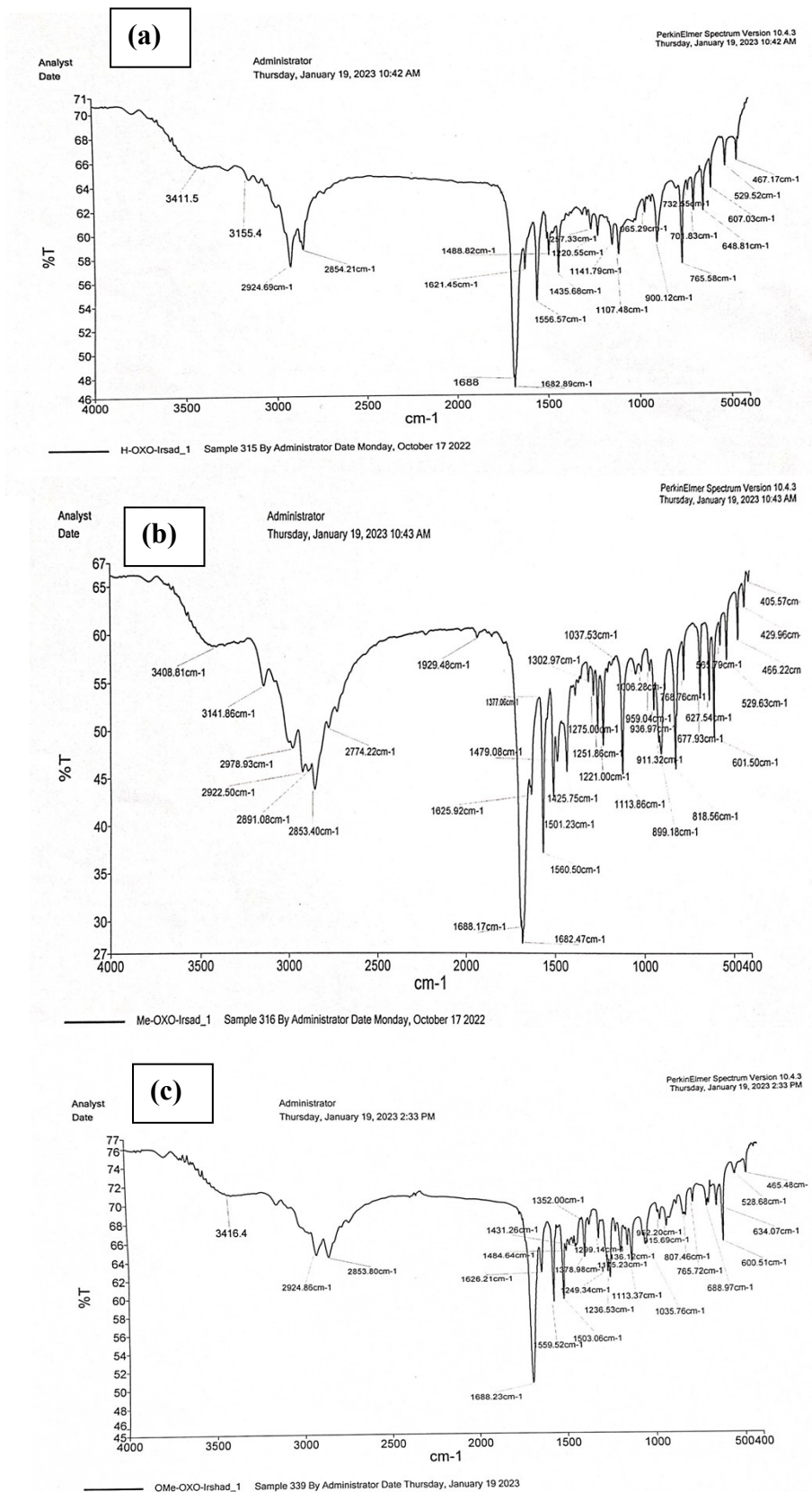


Fig. S7 IR spectra of A1 (a), A2 (b) and A3 (c).

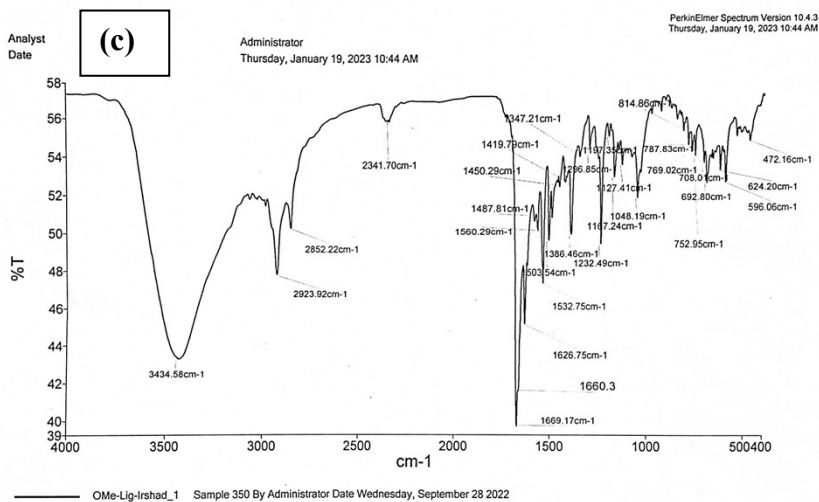
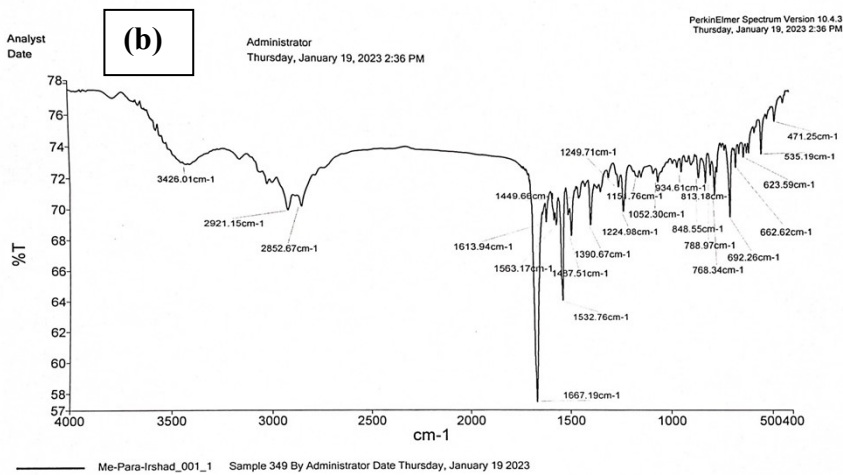
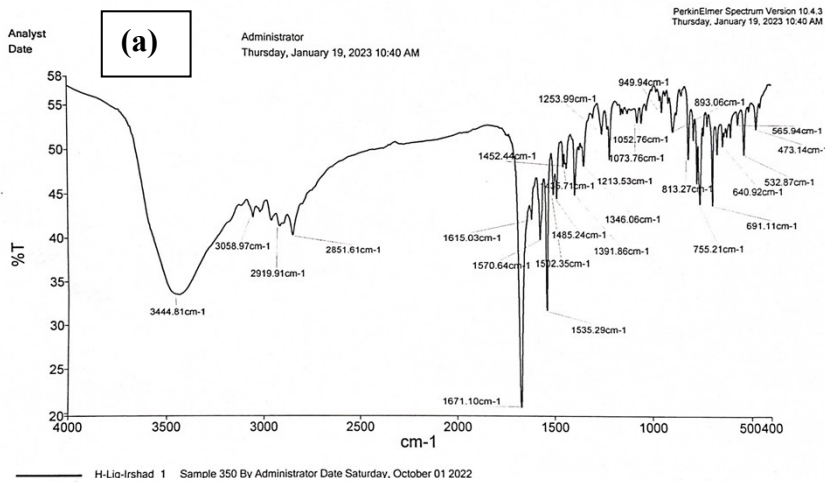


Fig. S8 IR spectra of Q1 (a), Q2 (b) and Q3 (c).

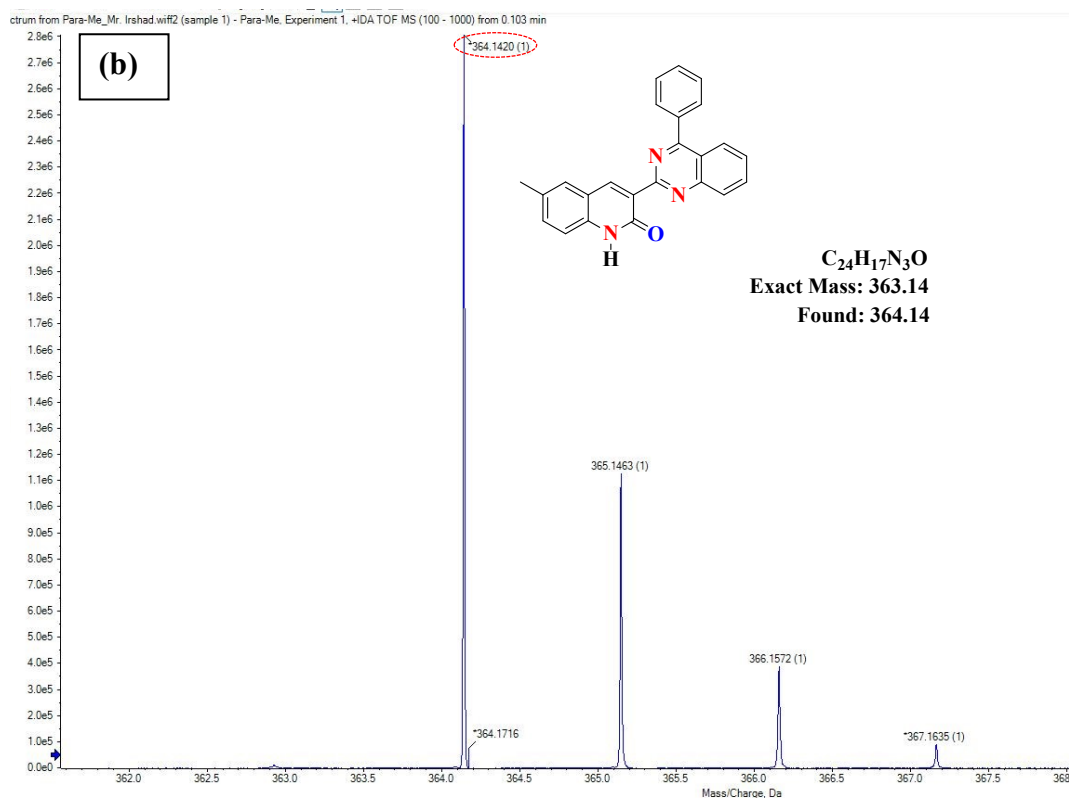
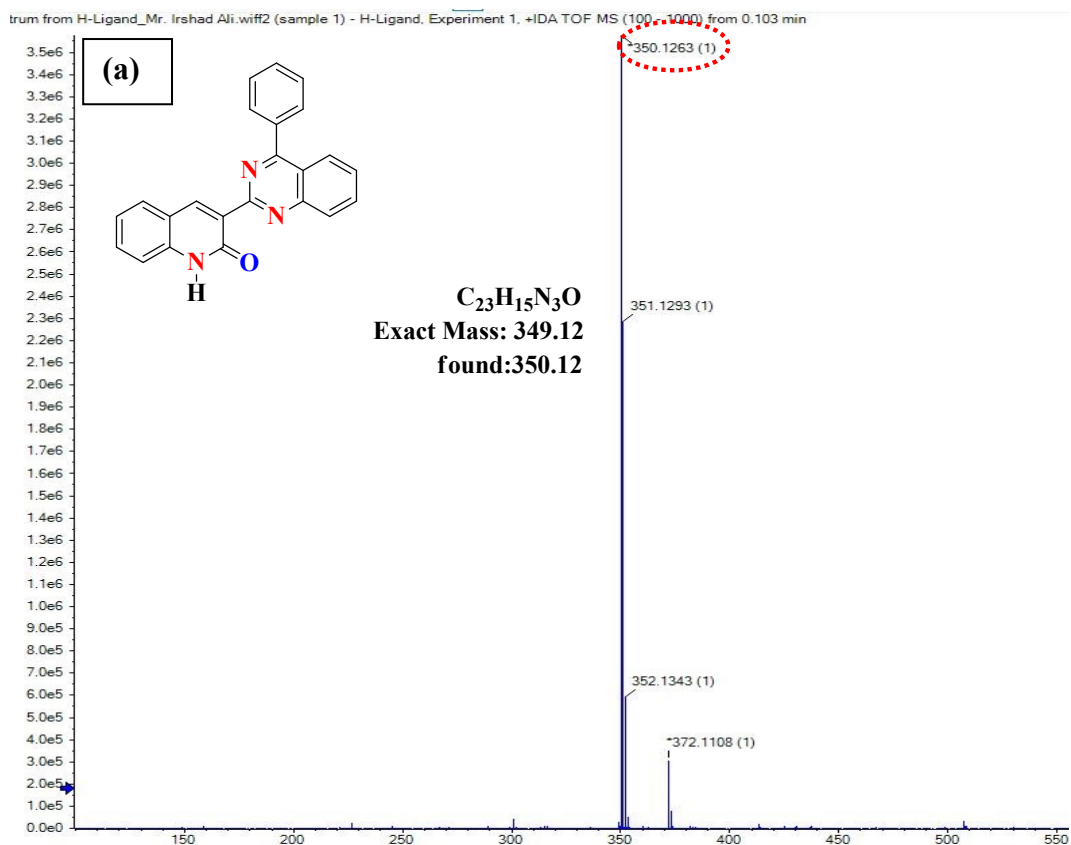


Fig. S9 HRMS spectra of **Q1** (a) and **Q2** (b).

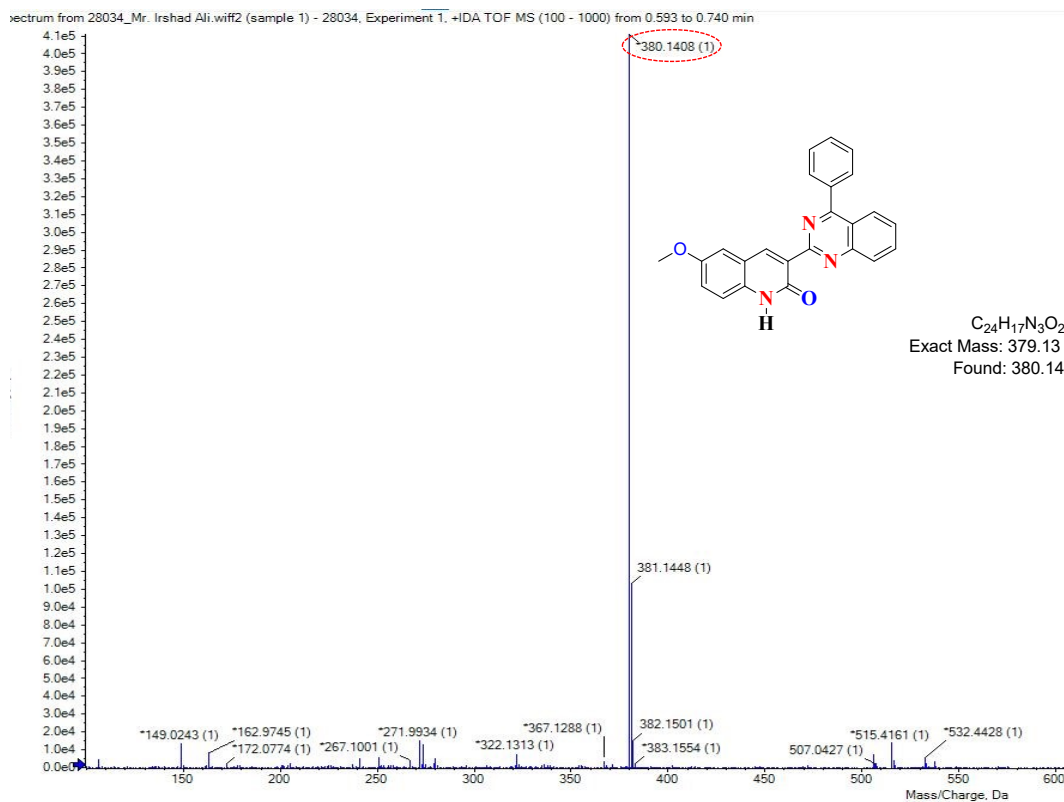


Fig. S10 HRMS spectrum of **Q3**.

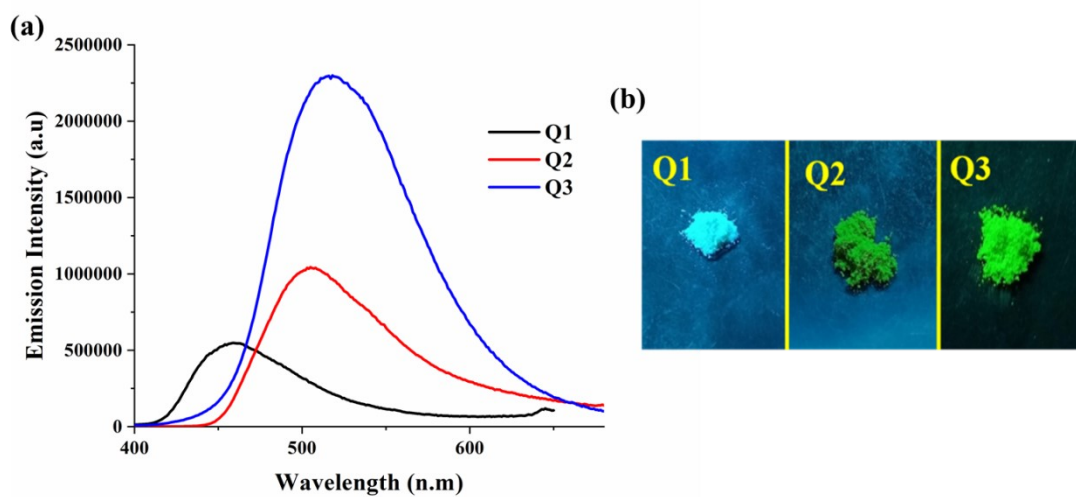


Fig. S11 (a) Solid-state emission spectrum of **Q1**, **Q2**, and **Q3** (λ_{ex} = 337, 358, and 385 nm, respectively). (b) **Q1–Q3** under the UV radiation of 365 nm.

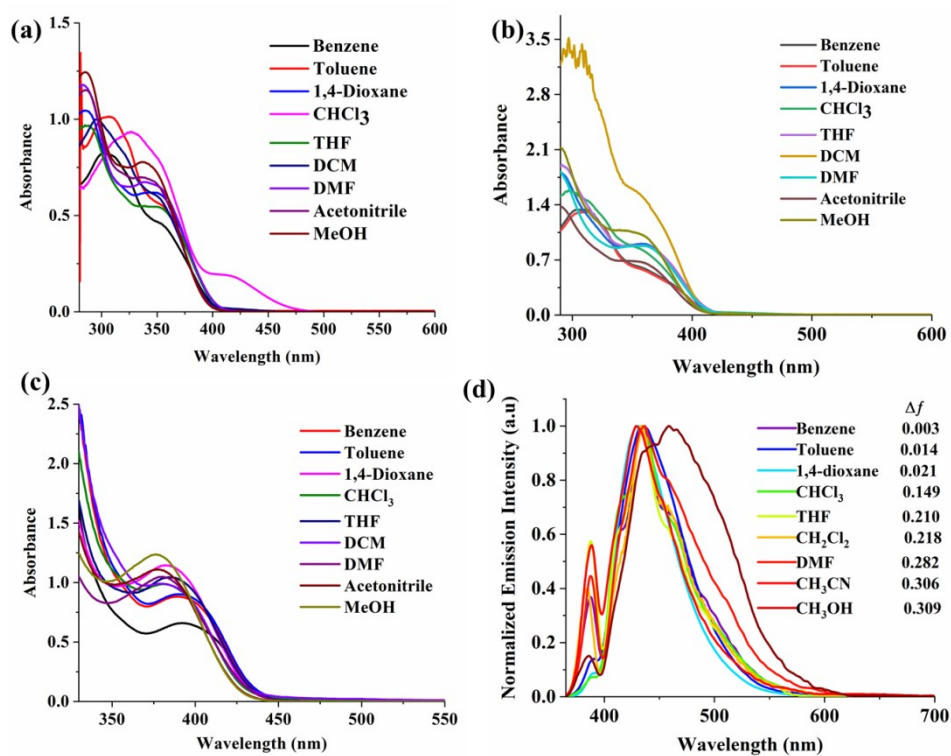


Fig. S12 Absorption spectra of **Q1** (a), **Q2** (b), **Q3** (c) and emission spectrum of **Q1** (d) in solvents ($c = 50 \mu\text{M}$) of varying polarity.

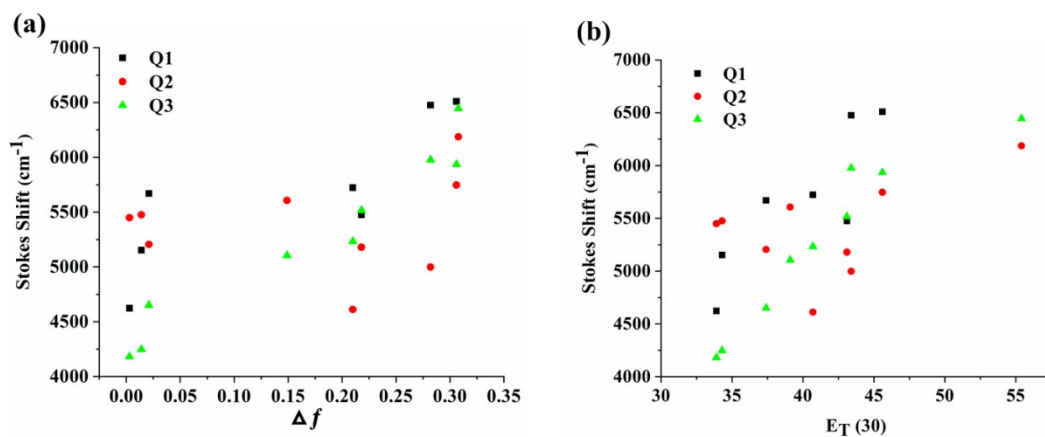


Fig. S13 Plots between (a) Stokes shift vs. Δf and Stokes shift vs. $E_T(30)$ (b).

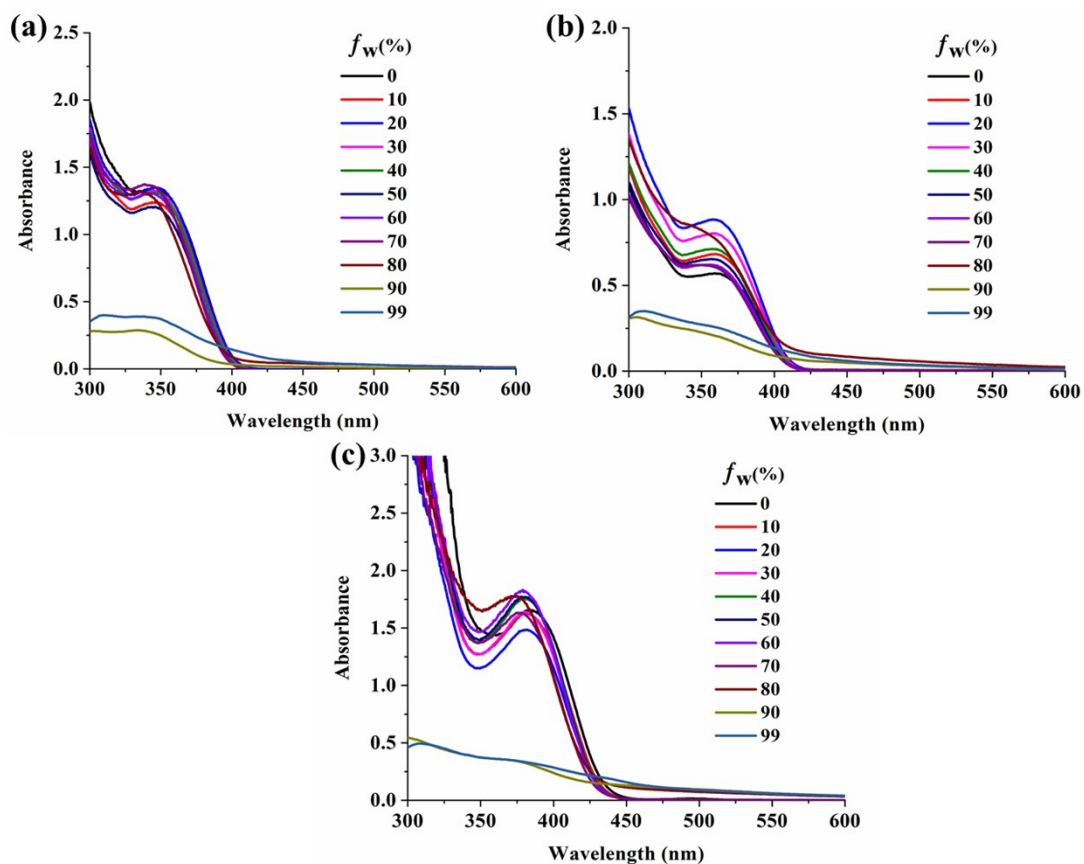


Fig. S14 Absorption spectra of **Q1** (a), **Q2** (b) and **Q3** (c) in THF/water ($c = 50 \mu\text{M}$).

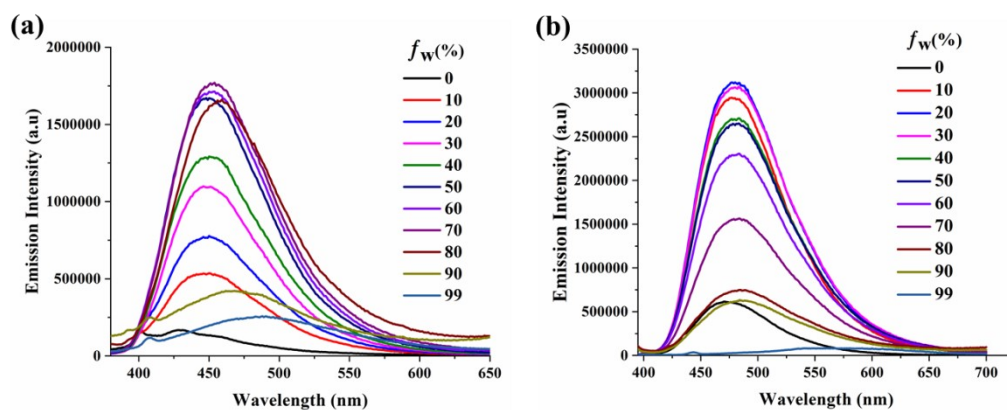


Fig. S15 Emission spectra of **Q2** (a), and **Q3** (b) in THF/water ($c = 50 \mu\text{M}$).

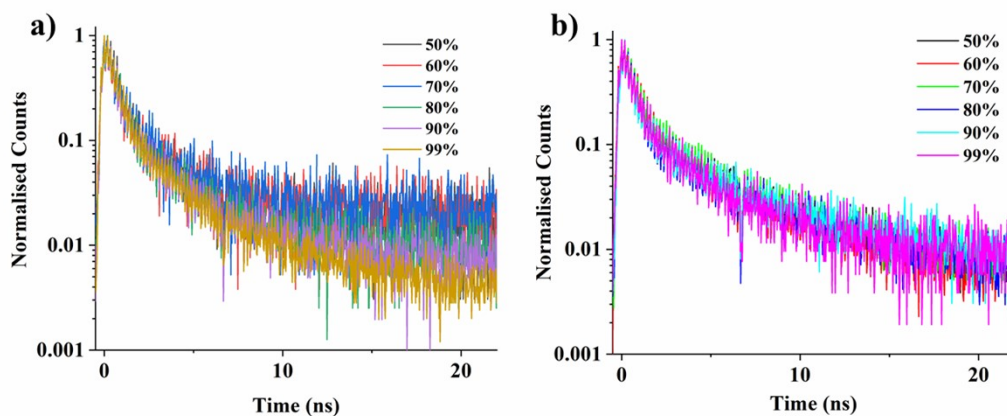


Fig. S16 A logarithmic view of the time-resolved fluorescence of Q2 (a), Q3 (b) in THF/water mixture ($c = 50 \mu\text{M}$).

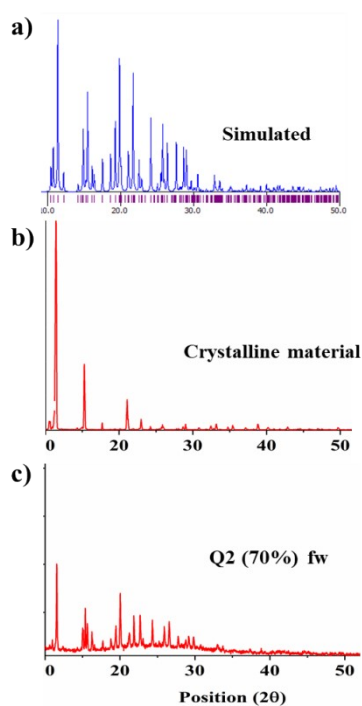


Fig. S17 Powder XRD Pattern of (a) Q2 simulated (b) crystalline material of Q2 (c) Q2 70% fw.

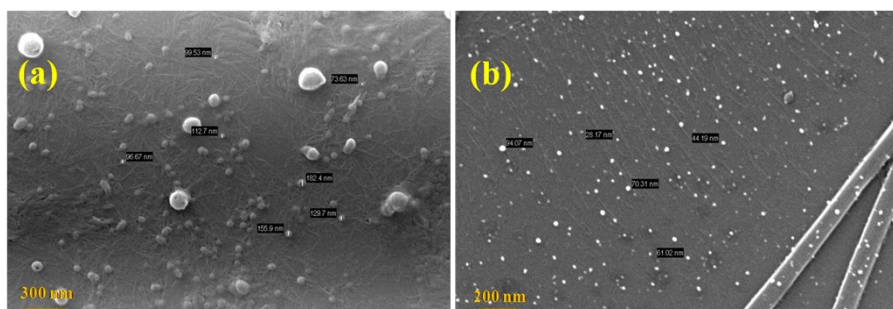


Fig. S18 SEM images of Q2 (a) and Q3 (b) in THF/water mixture.

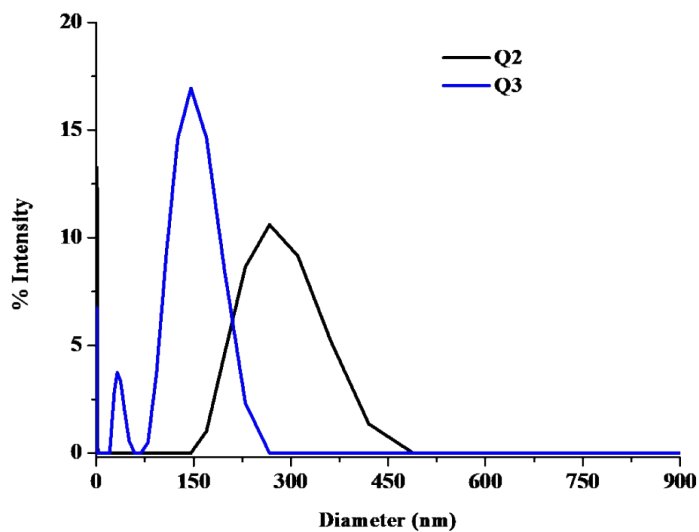


Fig. S19 Dynamic light scattering for **Q2** (70% fw) and **Q3** (90% fw) in THF/water mixture.

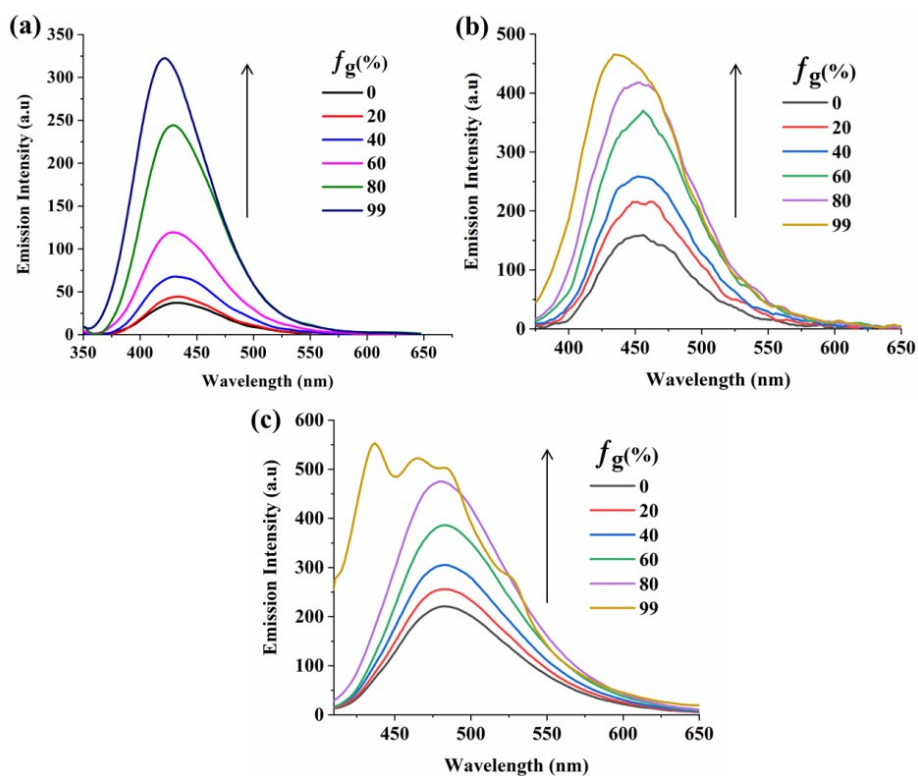


Fig. S20 Emission spectra of **Q1** (a), **Q2** (b) and **Q3** (c) in methanol/glycerol ($c = 50 \mu\text{M}$).

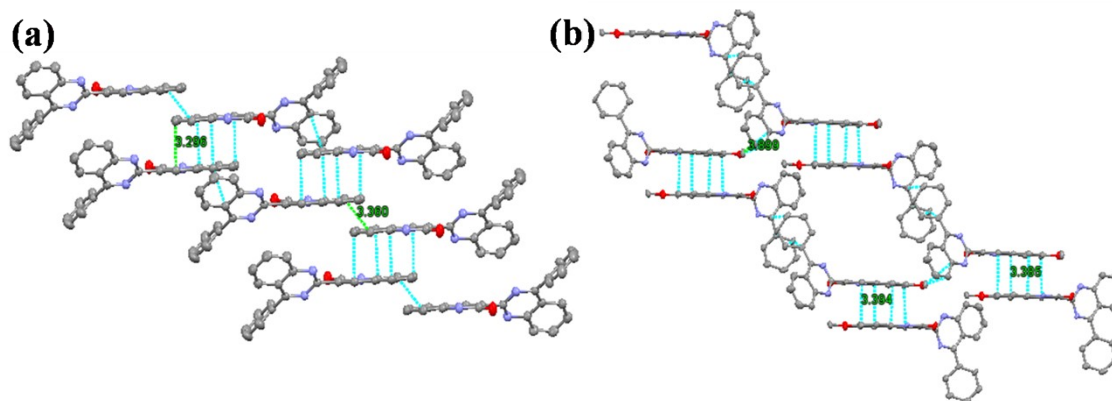


Fig. S21 Crystal packing of **Q1** (a), and **Q3** (b) through π - π stacking.

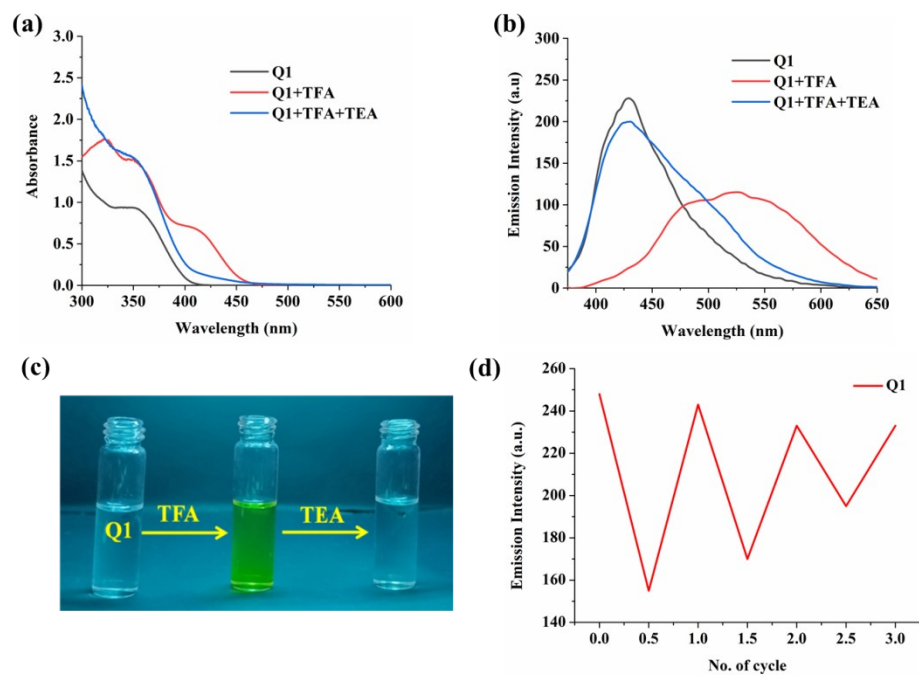


Fig. S22 (a) Absorption spectrum of **Q1**, **Q1+TFA** and **Q1+TFA+TEA**. (b) Emission spectrum of **Q1**, **Q1+TFA** and **Q1+TFA+TEA**. (c) Images of **Q1** ($c=5 \times 10^{-5}$ molL $^{-1}$) showing emission color changes after the addition of TFA and TEA, under the UV radiation of 365 nm. (d) Reversible switching of the emission of **Q1** by TFA/TEA cycle.

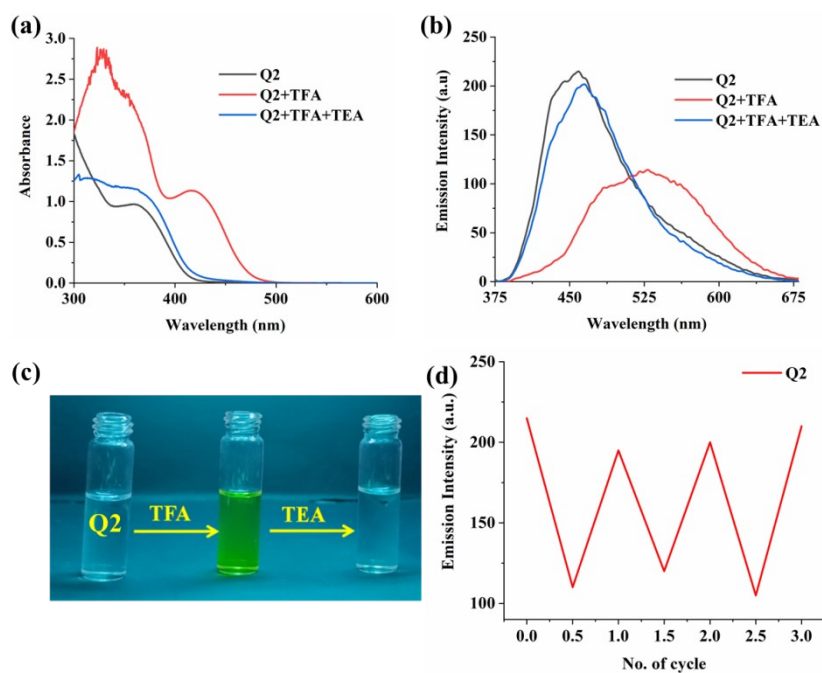


Fig. S23 (a) Absorption spectrum of **Q2**, **Q2+TFA** and **Q2+TFA+TEA**. (b) Emission spectrum of **Q2**, **Q2+TFA** and **Q2+TFA+TEA**. (c) Images of **Q2** ($c=5 \times 10^{-5}$ molL $^{-1}$) showing emission color changes after the addition of TFA and TEA, under the UV radiation of 365 nm. (d) Reversible switching of the emission of **Q2** by TFA/TEA cycle.

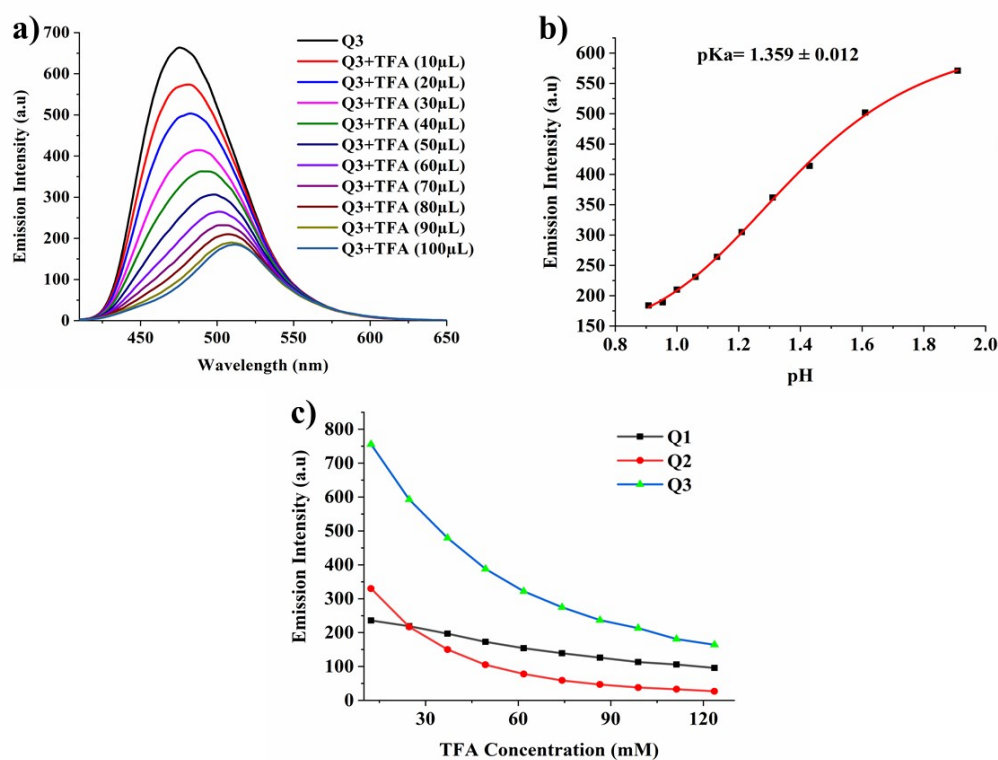


Fig. S24 (a) Emission spectrum of **Q3**, with addition of TFA (10-100 μ L) **Q3**+TFA (b) calculation of pKa by performing pH dependent fluorescence titration of **Q3** in THF (c; 50 μ M) at different pH (1.91, 1.61, 1.43, 1.31, 1.21, 1.13, 1.06, 1, 0.95, 0.90) (c) quantitative relationship between TFA concentration and emission intensity of **Q1**, **Q2**, and **Q3**.

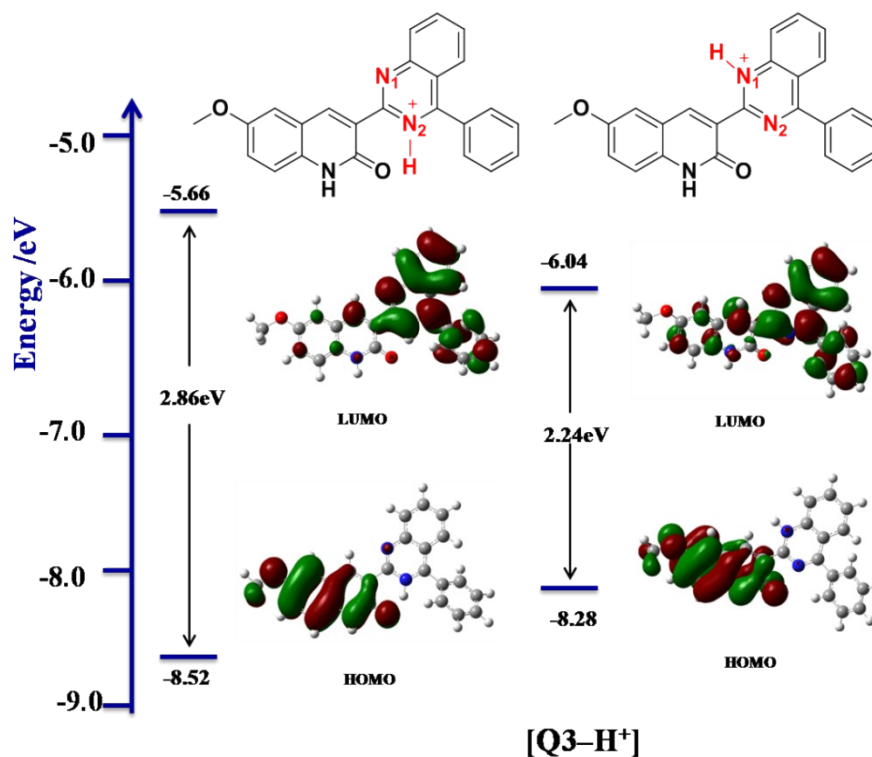


Fig. S25 DFT optimized structure of **[Q3-H⁺]**.

Table S1 Selected bond distances in **Q1**, **Q2** and **Q3**.

Q1	Bond Length (Å)	Q2	Bond Length (Å)	Q3	Bond Length (Å)
O1-C23	1.2363(15)	O1-C10	1.243(2)	O4-C10	1.237(8)
N1-C7	1.3189(16)	N2-C11	1.363(2)	O2-C34	1.245(9)
N1-C14	1.3613(16)	N2-C14	1.325(2)	O1-C26	1.371(9)
N2-C14	1.3140(16)	N1-C5	1.383(2)	O1-C25	1.387(9)
N2-C13	1.3726(16)	N1-C10	1.364(2)	O3-C2	1.356(10)
N3-C23	1.3635(16)	N3-C11	1.311(2)	O3-C1	1.414(8)
N3-C22	1.3806(17)	N3-C12	1.365(2)	N4-C29	1.390(9)
C7-C8	1.4249(18)	C11-C9	1.493(2)	N4-C34	1.366(8)

C7-C6	1.4875(17)	C9-C8	1.347(2)	N1-C10	1.356(8)
C8-C13	1.4098(18)	C9-C10	1.456(3)	N1-C7	1.404(9)
C8-C9	1.4147(18)	C5-C6	1.401(3)	N6-C35	1.366(9)
C17-C16	1.4292(17)	C5-C4	1.387(2)	N6-C42	1.335(9)
C17-C22	1.3981(18)	C6-C8	1.426(3)	N5-C35	1.301(9)
C17-C18	1.4042(18)	C6-C7	1.403(2)	N5-C36	1.355(9)
C14-C15	1.4809(17)	C14-C13	1.427(3)	N3-C11	1.374(9)
C15-C23	1.4668(17)	C14-C15	1.482(3)	N3-C18	1.317(9)
C15-C16	1.3525(17)	C13-C12	1.417(3)	N2-C11	1.292(8)
C6-C1	1.3861(19)	C13-C21	1.414(3)	N2-C12	1.388(8)
C6-C5	1.376(2)	C15-C16	1.398(3)	C35-C33	1.490(9)

Table S2 Selected bond angles in **Q1**, **Q2** and **Q3**.

Q1	Bond angle (°)	Q2	Bond angle (°)	Q3	Bond angle (°)
C14-N1-C7	117.84(11)	C14-N2-C11	117.68(16)	C1-O3-C2	117.6(6)
C13-N2-C14	116.29(11)	C10-N1-C5	125.33(18)	C7-N1-C10	125.0(6)
C22-N3-C23	125.56(12)	C12-N3-C11	116.17(16)	C18-N3-C11	118.3(6)
C8-C7-N1	121.52(12)	N3-C11-N2	126.92(17)	C12-N2-C11	117.3(6)
C6-C7-N1	115.14(11)	C9-C11-N2	114.84(16)	N2-C11-N3	125.8(6)
C6-C7-C8	123.05(11)	C9-C11-N3	118.17(16)	C9-C11-N3	114.5(6)
C13-C8-C7	115.93(11)	C8-C9-C11	120.37(16)	C9-C11-N2	119.7(6)
C9-C8-C7	124.80(12)	C10-C9-C11	118.78(17)	C12-C17-C18	116.7(7)
C9-C8-C13	119.00(12)	C10-C9-C8	120.84(17)	C16-C17-C18	125.5(7)
C22-C17-C16	117.60(11)	C6-C5-N1	119.12(17)	C16-C17-C12	117.7(7)
C18-C17-C16	123.72(12)	C4-C5-N1	121.25(17)	N1-C10-O4	121.4(7)
C18-C17-C22	118.64(12)	C4-C5-C6	119.62(18)	C9-C10-O4	122.7(6)
N2-C14-N1	126.49(12)	C8-C6-C5	117.24(17)	C9-C10-N1	115.9(6)
C15-C14-N1	116.16(11)	C7-C6-C5	118.78(18)	C4-C7-N1	120.5(7)
C15-C14-N2	117.34(11)	C7-C6-C8	123.98(18)	C6-C7-N1	118.6(6)
C23-C15-C14	118.39(11)	C13-C14-N2	120.96(17)	C6-C7-C4	120.8(7)

C16-C15-C14	121.63(11)	C15-C14-N2	115.93(16)	C10-C9-C11	119.2(6)
C16-C15-C23	119.84(12)	C15-C14-C13	123.10(17)	C8-C9-C11	120.0(7)
N3-C23-O1	120.28(12)	C6-C8-C9	122.23(18)	C8-C9-C10	120.7(6)
C15-C23-O1	124.23(12)	C12-C13-C14	116.06(17)	C3-C4-C7	119.5(7)
C15-C23-N3	115.46(11)	C21-C13-C14	125.26(17)	C8-C6-C7	117.6(7)
C1-C6-C7	117.20(12)	C21-C13-C12	118.62(17)	C5-C6-C7	118.4(7)
C5-C6-C7	123.66(13)	N1-C10-O1	120.80(18)	C5-C6-C8	124.0(7)
C5-C6-C1	119.14(13)	C9-C10-O1	124.02(18)	C2-C3-C4	121.0(7)
C15-C16-C17	122.51(12)	C9-C10-N1	115.17(18)	C17-C18-N3	120.9(7)
C17-C22-N3	118.89(12)	C16-C15-C14	118.77(17)	C19-C18-N3	115.2(6)
C21-C22-N3	120.68(12)	C20-C15-C14	122.87(18)	C19-C18-C17	123.9(7)
C21-C22-C17	120.41(12)	C20-C15-C16	118.27(17)	C6-C8-C9	122.2(7)
C8-C13-N2	121.87(11)	C13-C12-N3	121.98(17)	C20-C19-C18	122.6(7)
C12-C13-N2	118.81(12)	C24-C12-N3	118.70(18)	C24-C19-C18	117.5(7)
C12-C13-C8	119.17(12)	C24-C12-C13	119.27(19)	C24-C19-C20	119.8(7)

Table S3 Molar extinction coefficient (ϵ) for **Q1**, **Q2**, and **Q3** (c; 50 μ M)

Compounds	Absorption maxima	Molar extinction Coefficient (ϵ)
Q1	337	$2.40 \times 10^5 \text{ M}^{-1} \text{ cm}^{-1}$
Q2	358	$2.35 \times 10^5 \text{ M}^{-1} \text{ cm}^{-1}$
Q3	385	$2.09 \times 10^5 \text{ M}^{-1} \text{ cm}^{-1}$

Table S4 Emission maxima (λ_{em}) in the solid-state for **Q1**, **Q2**, and **Q3**.

Compounds	Emission maxima (THF solution)	Emission maxima (Solid state)
Q1	433	459
Q2	440	505
Q3	463	518

Table S5 Absorption and emissions maxima for **Q1**, **Q2**, and **Q3** in THF/water mixtures.

Water (vol %)	Q1		Q2		Q3	
	λ_{ab}/nm	λ_{em}/nm	λ_{ab}/nm	λ_{em}/nm	λ_{ab}/nm	λ_{em}/nm
0	337	401	358	429	385	465
10 to 80	346	438	355	450	382	483
90	306-333	480	303-358	462	285-298	488
99	309-337	499	311-358	490	286-305	-----

Table S6 Fluorescence quantum yield (Φ_f) for **Q1** at different water fractions (f_w) in THF/water mixtures.

Water fraction (vol %)	Fluorescence quantum yield (Φ_f) Q1
0%-40%	0.005
50%-60%	0.010
70%	0.013
80%	0.022
90%	0.191
99%	0.073

Fluorescence quantum yield (Φ_f) for **Q1** have been calculated relative to quinine sulphate (THF, $\lambda_{ex} = 310$ nm, $\lambda_{em} = 358$ nm, $\Phi = 0.55$) as a reference using the formula $[(\Phi = \Phi_R \times (I_T/I_R) \times (A_R/A_T) \times (\eta_T^2 / \eta_R^2)]$, where Φ = quantum yield, I = area under the curve of emission spectrum, A = absorbance at λ_{ex} , η = refractive index of solvent; The subscript R and T denote values for the reference and test samples respectively. Stock solutions for **Q1** have been prepared in THF; error $\pm 5\%$.

Table S7 Average life time ($\tau_{avg.}$) for **Q1** at water fractions (f_w) from 50%-99% in THF/water mixtures.

Q1 (Water vol %)	τ_1 (ns)	τ_2 (ns)	A1	A2	$\tau_{avg.}$	R ²
50	0.272	2.328	0.685	0.091	0.515	0.888

60	0.446	2.918	0.724	0.060	0.546	0.917
70	0.444	2.210	0.702	0.074	0.612	0.935
80	0.433	2.479	0.617	0.149	0.751	0.914
90	0.811	2.315	0.629	0.219	1.199	0.923
99	0.607	2.168	0.689	0.189	0.943	0.927

Table S8 Average life time ($\tau_{\text{avg.}}$) for **Q2** at water fractions (f_w) from 50%-99% in THF/water mixtures.

Q2 (Water vol %)	τ_1 (ns)	τ_2 (ns)	A1	A2	$\tau_{\text{avg.}}$	R²
50	0.437	2.789	0.671	0.092	0.722	0.902
60	0.499	3.246	0.736	0.073	0.748	0.935
70	0.413	2.360	0.609	0.132	0.871	0.907
80	0.399	2.609	0.596	0.101	0.720	0.918
90	0.468	2.925	0.727	0.078	0.708	0.924
99	0.336	1.854	0.550	0.163	0.684	0.889

Table S9 Average life time ($\tau_{\text{avg.}}$) for **Q3** at water fractions (f_w) from 50%-99% in THF/water mixtures.

Q3 (Water vol %)	τ_1 (ns)	τ_2 (ns)	A1	A2	$\tau_{\text{avg.}}$	R²
50	0.515	3.95	0.668	0.118	1.033	0.924
60	0.487	4.135	0.713	0.104	0.953	0.928
70	0.428	2.586	0.560	0.150	0.885	0.926
80	0.341	2.803	0.533	0.132	0.830	0.911
90	0.478	2.829	0.651	0.113	0.822	0.920
99	0.361	3.066	0.585	0.115	0.806	0.919